

REPORT DOCUMENTATION PAGE

Form Approved
OMB No. 0704-0188

The public reporting burden for this collection of information is estimated to average 1 hour per response, including the time for reviewing instructions, searching existing data sources, gathering and maintaining the data needed, and completing and reviewing the collection of information. Send comments regarding this burden estimate or any other aspect of this collection of information, including suggestions for reducing the burden, to the Department of Defense, Executive Service Directorate (0704-0188). Respondents should be aware that notwithstanding any other provision of law, no person shall be subject to any penalty for failing to comply with a collection of information if it does not display a currently valid OMB control number.

PLEASE DO NOT RETURN YOUR FORM TO THE ABOVE ORGANIZATION.

1. REPORT DATE (DD-MM-YYYY) 12-03-2012		2. REPORT TYPE Final		3. DATES COVERED (From - To) 1 DEC 2007 - 30 NOV 2010	
4. TITLE AND SUBTITLE Microscale convective heat transfer for thermal management of compact systems				5a. CONTRACT NUMBER	
				5b. GRANT NUMBER FA9550-08-1-0057	
				5c. PROGRAM ELEMENT NUMBER 61102F	
6. AUTHOR(S) Mohseni, Kamran				5d. PROJECT NUMBER	
				5e. TASK NUMBER	
				5f. WORK UNIT NUMBER	
7. PERFORMING ORGANIZATION NAME(S) AND ADDRESS(ES) University of Colorado - Boulder				8. PERFORMING ORGANIZATION REPORT NUMBER	
9. SPONSORING/MONITORING AGENCY NAME(S) AND ADDRESS(ES) AFOSR 875 N. Randolph St. Suite 325 Arlington, VA 22203				10. SPONSOR/MONITOR'S ACRONYM(S) AFOSR	
				11. SPONSOR/MONITOR'S REPORT NUMBER(S) AFRL-OSR-VA-TR-2012-0210	
12. DISTRIBUTION/AVAILABILITY STATEMENT Dist A					
13. SUPPLEMENTARY NOTES					
14. ABSTRACT The development of powerful and compact electronics has taxed current thermal management systems to their limit. However, electronic performance is closely related to operating temperature and thus improvements in cooling systems can greatly improve the performance of many components. The effects of digitized heat transfer using electrowetting on a dielectric were investigated in this paper. It was found that droplets maintained higher Nusselt numbers than continuous low and exhibited oscillations correlated to the circulation length which dampened out over time. Furthermore, droplets displayed heat transfer characteristics that were heavily dependent on the aspect ratio of the droplet where higher aspect ratios exhibited higher Nusselt numbers. In all cases, droplet Nusselt number was greater than the continuous Graetz flow. Using the results found here, droplet paths					
15. SUBJECT TERMS					
16. SECURITY CLASSIFICATION OF:			17. LIMITATION OF ABSTRACT UU	18. NUMBER OF PAGES 12	19a. NAME OF RESPONSIBLE PERSON Kamran Mohseni
a. REPORT U	b. ABSTRACT U	c. THIS PAGE U			19b. TELEPHONE NUMBER (Include area code) 352-273-1834

Reset

Microscale Convective Heat Transfer for Thermal Management of Compact Systems

FA9550-08-1-0057

PI: Kamran Mohseni

Department of Aerospace Engineering Sciences
University of Colorado at Boulder

1 Introduction

Modern electronics evolve to become more compact and more powerful everyday. However, an unresolved problem with these devices is adequate thermal management which limits technological advancement.[1] Examples of prolific heat generation are apparent anywhere from personal computer CPU's to high power lasers and micro-scale avionics. The generation of heat is unavoidable and has serious repercussions such as reduced functionality or catastrophic failure. Other effects of inadequate thermal management include increased signal noise in a semiconductor through the increased movement of free electrons. Regardless of these issues, engineers continue to strive for more powerful and compact electronic devices. It has been predicted that in the future, devices will generate heat at a rate greater than $250 \frac{W}{cm^2}$. [2, 3] Existing forms of thermal management are not capable of handling this amount of heat generation and thus the deficient heat transfer technology has throttled the advancement of high powered electronics[1].

Currently, the most commonly used thermal management systems consists of air cooled heat sinks attached to heat generating devices. One of the clear limiting factors of the existing system is the use of air which has a relatively high thermal resistance when compared to liquids and metals. By changing the cooling fluid to a liquid or metal, significantly higher heat transfer rates can be achieved. Liquid cooling has been a known option some time, and was first examined by Tuckerman and Pease[4] who implemented liquid cooling through microchannels. In recent years, additional methods of cooling have been investigated such as microjet devices[5], thermionic cooling[6][7] and thermoelectric microcoolers[8]. Additional information on microchannel transport has been presented by Garimell and Sobhan[9]. Information on liquid metal cooling has been presented by Miner and Ghosal[10].

In addition to the limitations of air, existing systems don't address hot spots. In any system, uneven distributions of heat are generated on a surface creating areas of elevated temperature, or hot spots. In existing systems these heat spikes are not specifically treated, resulting in cooling inefficiencies. In an ideal system, the hot spots that are generated would be treated on an individual basis without affecting other normally functioning areas. Unfortunately, specifically targeting hot spots is not realizable for continuous air or liquid flows.

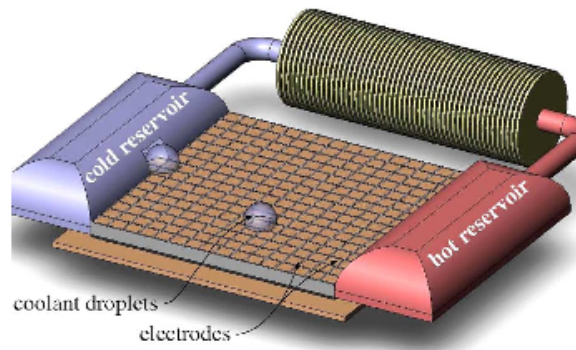
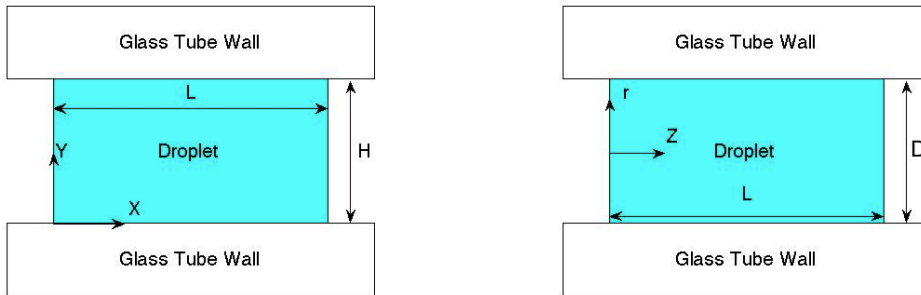


Figure 1: ELECTROWETTING ON A DIELECTRIC CONFIGURATION



(a) Parallel plate schematics.

(b) Axisymmetric plate schematics.

Figure 2: SCENARIO SCHEMATICS

An efficient and effective method of thermal management that exists is Digitized Heat Transfer (DHT)[11]. Digitized Heat Transfer refers to an array of discrete microdroplets that are used to "digitally" transfer heat away from the source. The microdroplets can consist of water, oil or even an liquid alloy. DHT using a liquid alloy coupled with Electrowetting on a Dielectric (EWOD)[11, 12, 13, 14] has been proposed by Mohseni. In comparison to air, all of these fluids have significantly higher thermal conductivities making them ideal for cooling systems[15]. In a simple configuration, a series of microdroplets could be transported evenly over a hot surface thus creating a continuously cooled system. In more complex systems, EWOD can be used to specifically address hot spots on an individual basis. In both cases, the microdroplet will originate from a cold reservoir, absorb heat at the hot surface, and exit to a hot reservoir where the fluid is cooled and then returned to the cold reservoir. Figure 1 shows a schematic for a simple DHT device with EWOD actuation of the droplets.

EWOD is a process in which a grid of electrodes is patterned onto a surface. To move a droplet, an electrostatic force is applied near the leading edge of the droplet through the generation of an electric field that is transverse to the direction of travel.[16, 17] There are numerous advantages to this system over traditional cooling systems or microchannels. First of all, the electrodes can be patterned onto any desired surface. Droplets can be transported on the top or bottom of a hot component without any issues. Additionally, there are no moving parts. Systems that consist of many moving parts have a tendency to break, and the lack of parts associated with EWOD is a clear advantage. Lastly, the grid like nature of EWOD lends itself to simple individualized commands that can be organized into complex sequences that will efficiently and effectively cool a surface. EWOD has been shown that it can be a reliable and efficient method for moving electrically conductive droplets[18, 19, 20] making the combination of DHT and EWOD a promising prospect for future thermal management.

Digitized heat transfer has many advantages over conventional continuous flow methods. The fluid properties of water or liquid metals are more conducive to high heat transfer rates and the individual droplets can be controlled to address specific heat spikes as they arise. However, the internal flow of the fluid has not been thoroughly investigated yet. This paper aims to examine the capabilities of digitized heat transfer from a numerical and experimental perspective.

MODEL

Governing Equations

The numerical model in this paper is governed by the incompressible continuity, momentum, and energy equations listed in Eq. (1) - Eq. (3). It is assumed that the scale of the flows are small enough that surface tension forces dominate and gravity can be considered negligible. Figure 2 shows the geometry and the axes that were defined for a parallel plate and axisymmetric scenario.

$$\frac{\partial u}{\partial x} + \frac{\partial v}{\partial y} = 0 \quad (1)$$

$$\rho \left(\frac{\partial \mathbf{v}}{\partial t} + \mathbf{v} \cdot \nabla \mathbf{v} \right) = -\nabla p + \mu \nabla^2 \mathbf{v} + \mathbf{f} \quad (2)$$

$$\rho \left(\frac{\partial T}{\partial t} + \mathbf{v} \cdot \nabla T \right) = \alpha \nabla^2 T \quad (3)$$

The calculations were done in terms of non dimensional variables. In the parallel plate flow, the variables were non dimensionalized using the following relations which were originally proposed by Baird[21].

$$u^* = \frac{u}{U} \quad x^* = \frac{x}{L} \quad y^* = \frac{y}{H} \quad t^* = \frac{tU}{H} \quad p^* = \frac{p + p_\infty}{\rho U^2} \quad \theta = \frac{T_w - T}{T_w - T_0}$$

For the non dimensionalization of v , scaling analysis is used on the continuity equation, Eq. (4), with the definitions listed above.

$$\frac{\partial u^*}{\partial x^*} + \frac{\partial v^*}{\partial y^*} = 0 \quad (4)$$

This yields Eq. (5) which provides a scaling for v .

$$\frac{U}{L} \sim \frac{V}{H} \Rightarrow V \sim \frac{UH}{L} \quad (5)$$

As a result, $v^* = \frac{VL}{UH}$. If a droplet is considered, there should only be a significant \underline{v} near the edges. As the droplet becomes longer and approaches a continuous flow, the effect of \underline{v} must disappear. The non dimensionalization of v accounts for this since a longer droplet will have a lower aspect ratio, $\frac{H}{L}$.

The non dimensional equations for a parallel plate flow are listed in Eq. (6) - Eq. (8) in addition to Eq. (4).

$$\begin{aligned} \frac{\partial u^*}{\partial t^*} + u^* \frac{H}{L} \frac{\partial u^*}{\partial x^*} + v^* \frac{H}{L} \frac{\partial u^*}{\partial y^*} \\ = -\frac{H}{L} \frac{\partial P^*}{\partial x^*} + \frac{1}{Re} \left(\frac{H^2}{L^2} \frac{\partial^2 u^*}{\partial x^{*2}} + \frac{\partial^2 u^*}{\partial y^{*2}} \right) \end{aligned} \quad (6)$$

$$\begin{aligned} \frac{\partial v^*}{\partial t^*} + u^* \frac{H}{L} \frac{\partial v^*}{\partial x^*} + v^* \frac{H}{L} \frac{\partial v^*}{\partial y^*} \\ = -\frac{L}{H} \frac{\partial P^*}{\partial y^*} + \frac{1}{Re} \left(\frac{H^2}{L^2} \frac{\partial^2 v^*}{\partial x^{*2}} + \frac{\partial^2 v^*}{\partial y^{*2}} \right) \end{aligned} \quad (7)$$

$$\frac{\partial \theta}{\partial t^*} + u^* \frac{H}{L} \frac{\partial \theta}{\partial x^*} + v^* \frac{H}{L} \frac{\partial \theta}{\partial y^*} = \frac{1}{Pe} \left(\frac{H^2}{L^2} \frac{\partial^2 \theta}{\partial x^{*2}} + \frac{\partial^2 \theta}{\partial y^{*2}} \right) \quad (8)$$

$$Pe = \frac{UH}{\alpha} \quad AR = \frac{H}{L} \quad Re = \frac{HU}{\nu}$$

For an axisymmetric pipe in cylindrical coordinates, the variables are non dimensionalized using the following definitions.

$$u_z^* = \frac{u_z}{U} \quad z^* = \frac{z}{L} \quad r^* = \frac{r}{D} \quad t^* = \frac{tU}{D} \quad p^* = \frac{p + p_\infty}{\rho U^2} \quad \theta = \frac{T_w - T}{T_w - T_0}$$

Using the same scaling analysis and the continuity equation, Eq. (9), the scaling factor for u_r was derived, Eq. (10)

$$\frac{1}{r} \frac{\partial(ru_r)}{\partial r} + \frac{\partial u_z}{\partial z} = 0 \quad (9)$$

$$\frac{1}{D} \frac{DU_r}{D} \sim \frac{U}{L} \Rightarrow U_r \sim \frac{UD}{L} \quad (10)$$

This yields $u_r^* = \frac{Lu_r}{UD}$. The cylindrical non-dimensional equations for the axisymmetric pipe are listed in Eq. (9) and Eq. (11) - Eq. (13).

$$\begin{aligned} \frac{\partial u_r^*}{\partial t^*} + u_r^* \frac{H}{L} \frac{\partial u_r^*}{\partial r^*} + u_z^* \frac{H}{L} \frac{\partial u_r^*}{\partial z^*} \\ = -\frac{L}{H} \frac{\partial P^*}{\partial r^*} + \frac{1}{Re} \left(\frac{1}{r^*} \frac{\partial u_r^*}{\partial r^*} + \frac{\partial^2 u_r^*}{\partial r^{*2}} + \frac{H^2}{L^2} \frac{\partial^2 u_r^*}{\partial z^{*2}} - \frac{u_r^*}{r^{*2}} \right) \end{aligned} \quad (11)$$

$$\begin{aligned} \frac{\partial u_z^*}{\partial t^*} + u_r^* \frac{H}{L} \frac{\partial u_z^*}{\partial r^*} + u_z^* \frac{H}{L} \frac{\partial u_z^*}{\partial z^*} \\ = -\frac{H}{L} \frac{\partial P^*}{\partial z^*} + \frac{1}{Re} \left(\frac{1}{r^*} \frac{\partial u_z^*}{\partial r^*} + \frac{\partial^2 u_z^*}{\partial r^{*2}} + \frac{H^2}{L^2} \frac{\partial^2 u_z^*}{\partial z^{*2}} \right) \end{aligned} \quad (12)$$

$$\begin{aligned} \frac{\partial \theta}{\partial t^*} + u_r^* \frac{H}{L} \frac{\partial \theta}{\partial r^*} + u_z^* \frac{H}{L} \frac{\partial \theta}{\partial z^*} \\ = \frac{1}{Pe} \left(\frac{1}{r^*} \frac{\partial \theta}{\partial r^*} + \frac{\partial^2 \theta}{\partial r^{*2}} + \frac{H^2}{L^2} \frac{\partial^2 \theta}{\partial z^{*2}} \right) \end{aligned} \quad (13)$$

This paper also compares the effectiveness of heat transfer which will be done through Nusselt number. For numerical results of the parallel plate simulation, Nusselt number is defined by Eq. (14).

$$Nu = \frac{\frac{\partial \theta}{\partial y^*}(x, 0)}{\theta_{avg}(x)} \quad (14)$$

$$\theta_{avg} = \int_0^1 \theta(x, y) \frac{u}{U} dy \quad (15)$$

For the numerical results of the axisymmetric simulation, Nusselt number is defined by Eq. (16).

$$Nu = \frac{-2 \frac{\partial \theta}{\partial r^*}(z, 1)}{\theta_w - \theta_b} \quad (16)$$

$$\theta_b = \frac{\int_0^1 (1 - r^{*2}) r^* \theta dr^*}{\int_0^1 (1 - r^{*2}) r^* dr^*} \quad (17)$$

In experimental tests, θ_{avg} is not a feasible measurement. It would be very difficult to fit a thermocouple in a microchannel and once in place it would have a negative effect on the flow of the droplet. Therefore the inlet temperature of the droplet is used instead of θ_{avg} producing Eq. (18).

$$Nu = \frac{Dq''}{k(T_w - T_0)} \quad (18)$$

Numerical Method

The Navier Stokes equations described above were numerically solved in MATLAB on a staggered grid based on a two dimensional Navier Stokes solver. The simulations in this paper only considered rectangular droplets. The nonlinear terms are treated explicitly with a centered differencing scheme. However, for faster flows or larger time steps, an upwind approach was taken. A CFL condition exists, which in turn limits the time step by a constant times the spacial resolution. The viscosity terms are treated implicitly and therefore there is no time step restriction. A pressure correction step is taken to enforce continuity in the flow field. By solving the poisson equation for pressure, and correcting the field to be divergent free, continuity is enforced.

Experimental Set Up and Procedure

An experiment was configured to verify the accuracy of the numerical model. The experiment can be separated into the droplet formation section and heated test section. In the droplet formation section, water and air are mixed to create droplets. Then the droplets pass into a heated section where they extract heat. Next the droplets exit the test section and are collected to verify droplet temperature and velocity calculations.

The droplet formation section consists of a T-shaped junction, a water reservoir and a gas line. In digitized heat transfer, different fluids can be used to transfer the heat, and based on preliminary examination, it is more efficient to use liquid metals. However in order to create a safe and easily repeatable experiment, water was used. Water is not as efficient as liquid metal, but still demonstrates the advantages of digitized heat transfer over conventional continuous air flow. The water droplets that are formed are created by the mixing of the two fluids at the junction. The test set up can be seen in Figure 3. By adjusting the flow rate of the water and the air, the flow rate, droplet size, and frequency can be adjusted. The velocity, size and frequency of the droplets were measured using a high speed camera. The air is regulated by a Numatics R880-02A air high flow precision regulator. The water is regulated by a Legris 7067 compact flow regulator. This simple method shows good flexibility and consistency.

The heated test section is composed of a glass tube, insulation, heating wires, and thermocouples as seen in the cross section shown by Figure 4. The inner diameter of the glass tube is 2.6 mm and has a wall thickness of 3.15 mm. In this section, a glass tube is heated and insulated while water droplets pass through the internal channel removing heat. NiCr wire was used to for the heating element, which is carefully wired to evenly distribute the heat along the test section. The temperature of the glass tube wall is measured by T-type, 40 gauge thermocouples in 1.2 mm diameter holes. The holes were drilled at two radial depths of 50% and 95% of wall thickness along the heated section and filled with silicon oil to ensure accurate thermal measurement. The thermocouples are connected to a Ni-SXCI-1102 thermocouple input module through a terminal block with cold junction compensation. The input module is connected to the NI data acquisition board through a NI-SCXI-1303 chassis board. Temperature data is recorded at 250 Hz. Along the glass tube, there are 12 distinct measurement points along the x axis within the heated section. Furthermore, there are thermocouples measuring the inlet and exit droplet temperature. Using the temperature data collected, it is possible to calculate the wall temperature and predict the Nusselt number at that axial location.



Figure 3: DROPLET FORMING T-JUNCTION

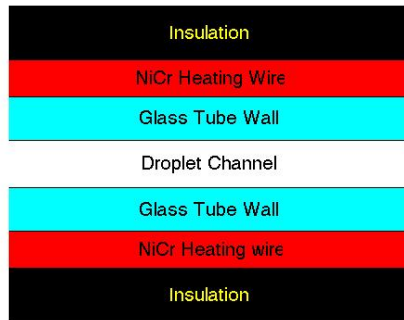


Figure 4: TEST SECTION

RESULTS

Numerical Results

The numerical simulations created for this paper were run for two dimensional parallel plate flow as well as axisymmetric pipe flow. Using the numerical method described above, steady state velocity field of the droplet was determined and is shown in Figure 5. This figure shows the streamlines from a reference frame moving with the droplet. It is clear that the droplet is divided symmetrically into two vortices that are rotating opposite each other. Near the edges, v is dominant which results in an increase in convective heat transfer. Figure 5 shows \underline{u} at various vertical cross sections in a non moving reference frame. The flow closer to the center of the droplet approaches a poiseuille velocity profile. At the edges of the droplet, \underline{u} approaches slug flow showing that the \underline{u} develops from a slug flow to a poiseuille flow and then back to a slug flow at the opposite edge. However, in droplets that have aspect ratios close to 1, the effects of the edges are more apparent in the \underline{u} velocity at the center and the flow never fully develops into a full poiseuille profile. As the aspect ratios is decreased, the effect of the edges of the droplet become less influential and \underline{u} is capable of reaching the fully developed poiseuille profile.

Figure 6 shows Nusselt number of various sized droplets where they are heated with constant wall temperature starting at $x = 0$. In Figure 6 the Nusselt number is plotted versus the x distance

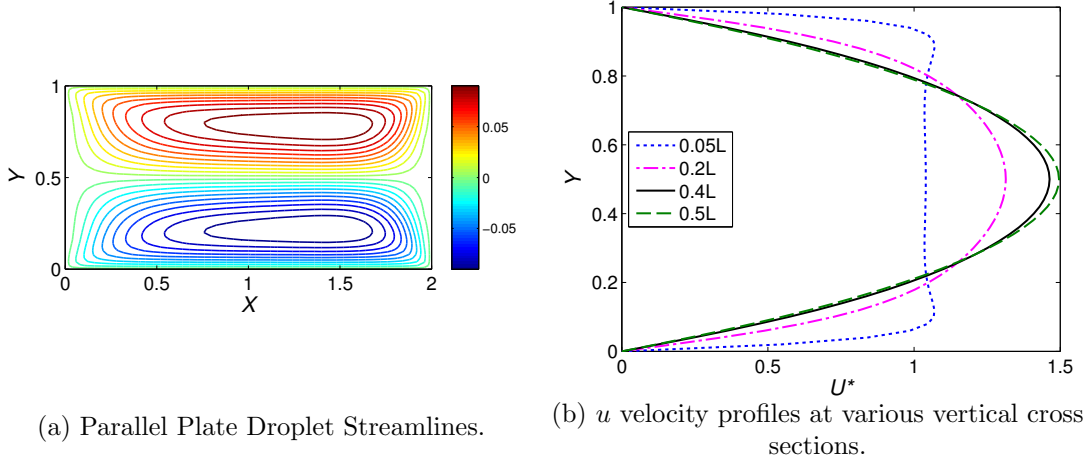


Figure 5: 2D DROPLET WITH $AR = 0.5$ AND $Re = 100$.

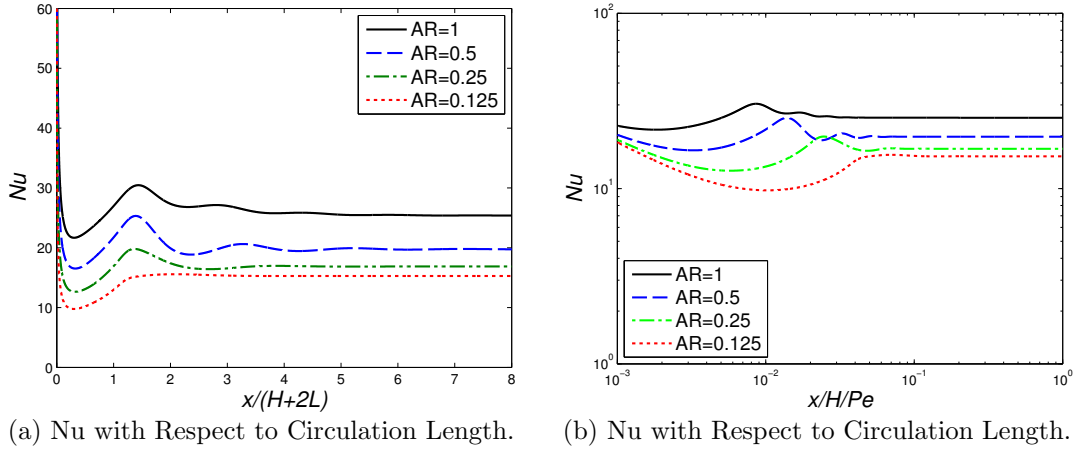


Figure 6: Nu OF DROPLET WITH $Re = 100$ AND $Pe = 500$.

traveled non dimensionalized by the circulation length. The circulation length is determined to be $H+2L$ because it is the distance a particle must travel if it starts in the a corner of the droplet and travels in a rectangular path until it reaches its original position. Figure6 shows the Nusselt number compared to the classic non dimensional length as used by Bejan.[22] In Figure 6, the oscillations in Nusselt number show a clear relation to the number of circulations that the droplet has experienced. Even in long droplets, there is a clear relationship between the Nusselt number and circulation. Furthermore, droplets with smaller aspect ratios display lower Nusselt numbers. This is an expected result since droplets with lower aspect ratios only have \underline{v} near the edges and the majority of the droplet is characterized by a poiseuille like profile. This can be further justified by looking at the physical meaning of Nu. Nu can physically be interpreted as a ratio of the convective heat transfer over the conductive heat transfer. Therefore, it is expected that a shorter droplet will have more circulation and a higher Nusselt number than longer droplets.

As the droplet continues to travel down the heated section the temperature difference between the droplet and wall decreases and the internal circulation begins to have a decreased effect. Droplets with smaller aspect ratios approach a steady Nu in less circulation lengths, but further distances down the heated section. The numerical results predict that a droplet with $AR = 0.125$ will reach

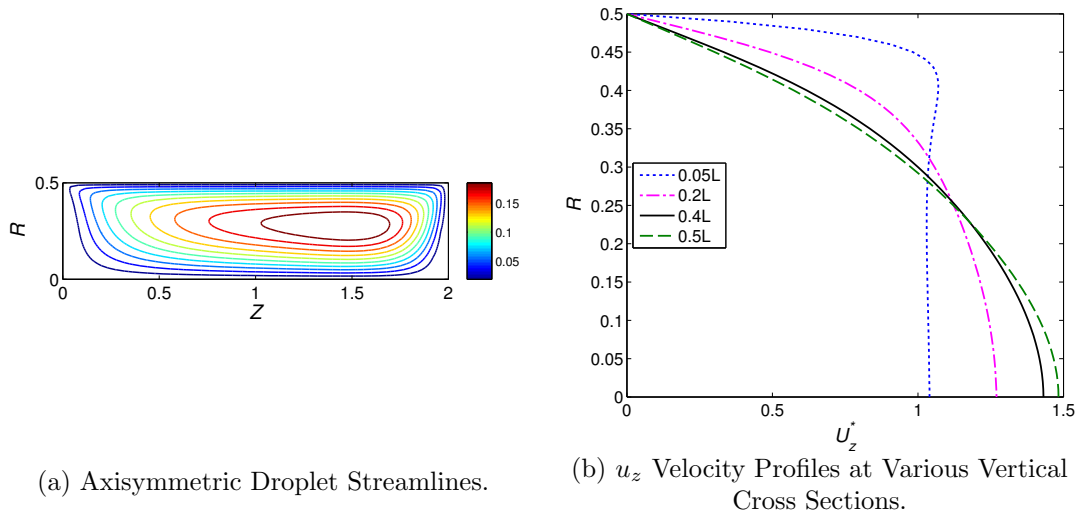


Figure 7: AXISYMMETRIC DROPLET STREAMLINES AR = 0.5 Re = 100.

its steady state Nusselt number in roughly 2 circulations, but a droplet with AR = 1 will take 4 to 5 circulations. On the other hand, the same droplet with AR = 0.125 will reach a steady Nu at roughly $x/H/Pe = 0.06$ where as the square droplet will reach its steady Nu at approximately $x/H/Pe = 0.02$.

Figure 6 shows the Nusselt number over a large distance. Even at a distance far away from the start of the heated section, where the droplet has been heated continuously, the Nusselt number maintains a steady state that is higher than the Graetz flow which asymptotes at a Nusselt number of 7.54.[22] However, at positions far down from the start of the heated section, the temperature difference between the wall and droplet is minimal and there is not a significant amount of heat transferred despite the higher Nusselt number. It is only a comparison of the convective heat transfer to the conductive heat transfer, as mentioned earlier.

The same code written by Seibold was modified for the axisymmetric pipe simulation. The streamlines for the axisymmetric case can be seen in Figure 7 and the associated u_z profiles are shown in Figure 7. The flow field for a droplet in an axisymmetric pipe is closely related to the predicted flow in between parallel plates. There are two counter rotating vortices on either side of the axis of symmetry and the velocity along the axis of symmetry approaches the Hagen-Poiseuille profile as the droplets become longer. Figure 8 shows the predicted Nusselt number for various length droplets subject to constant wall temperature.

As expected, the Nusselt number of an axisymmetric droplet displays many of the same characteristics as the parallel plate droplet. In Figure 8 the Nusselt number of a droplet with a high aspect ratio exhibits a higher Nusselt number. Like the parallel plate, this can be attributed to the short circulation length that causes an increase in convective heat transfer. Also, axisymmetric Nusselt number shows a similar dependency to the circulation length as seen in Figure 8. Droplets with an aspect ratio closer to one exhibit oscillations in Nusselt number for longer since convective heat transfer is more active. In droplets with lower aspect ratios, convective heat transfer is less prevalent and thus its Nusselt number reaches its steady state value more quickly. In Figure 8, a droplet with an aspect ratio of 0.125 takes roughly 3 circulation lengths to settle where as a droplet with an aspect ratio of 1 takes roughly 15 circulation lengths. The trend is similar to parallel plate droplets however axisymmetric droplets with a comparable aspect ratio will take more circulation lengths to dampen out the oscillations. Overall, droplets show a greater Nusselt number than the Graetz flow which asymptotes at a Nu of 3.66 for isothermal walls.[22]

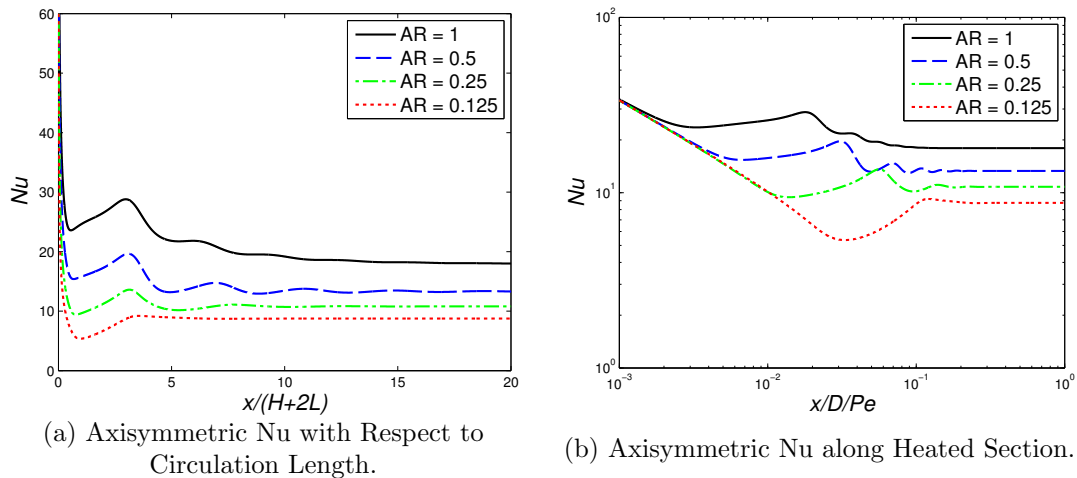


Figure 8: AXISYMMETRIC Nu OF DROPLET WITH $Re = 0.5$ AND $Pe = 500$

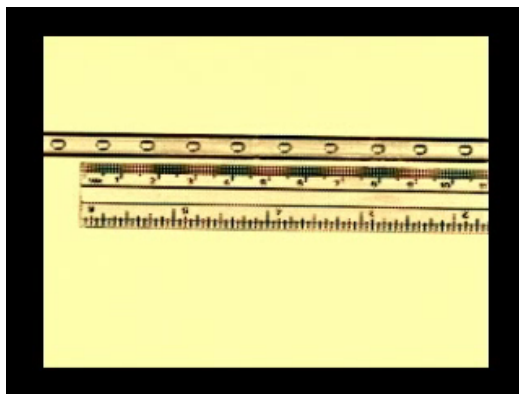


Figure 9: EXPERIMENTAL DIGITIZED FLOW

In the field of thermal management, these results could be useful in determining droplet paths. For example, if a hot spot were to arise, droplets could be translated to the site to remove the heat. If the path were arbitrarily determined, it might pass over the hot spot during a local min in the Nusselt number. However, if the droplet size and surface temperature is known, a path could be determined that would align a local peak in the Nusselt number with the hot spot.

EXPERIMENTAL RESULTS

Experimental tests are currently being run using the apparatus described in the Experimental Set up section. Preliminary tests show that the system is capable of producing droplet velocities as low as 4 cm/s while maintaining good control over droplet aspect ratio. A sample flow is shown in Figure 9. Furthermore, initial results show that digitized flow is capable of maintaining the same steady state temperature using smaller mass flow rates. The final draft will include a comparison of Nusselt number between experimental and numerical results as well as a comparison between digitized and continuous flow.

Conclusion

The development of powerful and compact electronics has taxed current thermal management systems to their limit. However, electronic performance is closely related to operating temperature and thus improvements in cooling systems can greatly improve the performance of many components. The effects of digitized heat transfer using electrowetting on a dielectric were investigated in this paper. It was found that droplets maintained higher Nusselt numbers than continuous flow and exhibited oscillations correlated to the circulation length which dampened out over time. Furthermore, droplets displayed heat transfer characteristics that were heavily dependent on the aspect ratio of the droplet where higher aspect ratios exhibited higher Nusselt numbers. In all cases, droplet Nusselt number was greater than the continuous Graetz flow. Using the results found here, droplet paths can be intelligently programmed so that peak Nusselt numbers are aligned with the hot spots. Electrowetting on a Dielectric in combination with Digitized heat transfer shows significant promise for thermal management applications. Future work will be focused on combining the two to optimally cool a surface.

References

- [1] S. Garmella, Y. Joshi, A. Bar-Cohen, A. Mahajong, K. Toh, V. Carey, M. Baellmans, J. Lohan, B. Sammakia, and F. Andros. Thermal challenges in next generation electronic systems - summary of panel presentations and discussions. IEEE Transactions on Components and Packaging Technologies, 25(4):569–575, 2002.
- [2] V. Singhal, S.V. Garimella, and A. Raman. Microchannel pumping technologies for microchannel cooling systems. Appl Mech Rev, 57(3):191–221, 2004.
- [3] Thermal Management Technology Roadmap of the National Electronics Manufacturing Initiative (NEMI). Office of the Secretary of Defense, 2002.
- [4] D.B. Tuckerman and R.F. Pease. High performance heat sinking for VLSI. IEEE Electron Device Letters, 2(5):126–129, 1981.
- [5] D.S. Kercher, J.-B. Lee, O. Brand, M.G. Allen, and A. Glezer. Microjet cooling devices for thermal management of electronics. Proceedings of IEEE Transactions on Components and Packaging Technologies, 26:359–366, June 2003.
- [6] A. Shakouri and J.E. Bowers. Heterostructure integrated thermionic coolers. Appl. Phys. Lett., 71(9):1234–1236, 1997.
- [7] A. Shakouri, C. Labounty, P. Abraham, J. Piprek, and J.E. Bowers. Enhanced thermionic emission cooling in high barrier superlattice heterostructures. In Material Research Society Symposium Proceedings, volume 545, pages 449–458, December 1998.
- [8] J. Fluerial, A. Borshcevsy, M. Ryan, W. Phillips, E. Kolawa, T. Kacisch, and R. Ewell. Thermoelectric microcoolers for thermal management applications. In Proceeding of the IEEE Conference on Thermoelectrics, pages 641–645, 1997.
- [9] S.V. Garimella and C.B. Sobhan. Transport in microchannels-a critical review. Annual Review of Heat Transfer, 13, 2003.
- [10] A. Miner and U. Ghosal. Cooling of high-power-density microdevices using liquid metal coolants. Appl. Phys. Lett., 85(3):506–508, 2004.
- [11] K. Mohseni, E. Baird, and H. Zhao. Digitized heat transfer for thermal management of compact microsystems. In Proceedings of the 2005 ASME International Mechanical Engineering Congress and R & D Expo, pages IMECE 2005–79372, Orlando, Florida, November 5-11 2005. ASME.
- [12] K. Mohseni. Effective cooling of integrated circuits using liquid alloy electrowetting. In Proceedings of the Semiconductor Thermal Measurement, Modeling, and Management Symposium (SEMI-Therm), San Jose, California, USA, March 15 - 17 2005. IEEE.
- [13] K. Mohseni and E. Baird. Digitized heat transfer using electrowetting on dielectric. Nanoscale and Microscale Thermophysical Engineering, 11(1 & 2):99 – 108, 2007.
- [14] K. Mohseni and E. Baird. Digitized heat transfer: Thermal management of compact micro systems using electrostatic droplet actuation. AIAA paper 2007-4157, 39th AIAA Thermophysics Conference, Miami, FL, June 25 - 28 2007.
- [15] V.K. Pamula and K. Chakrabarty. Cooling of integrated circuits using droplet-based microfluidics. In Proc. ACM Great Lakes Symposium on VLSI, pages 84–87, 2003.
- [16] E. Baird, P. Young, and K. Mohseni. Electrostatic force calculation for an EWOD-actuated droplet. To appear in Microfluid Nanofluid, 2007. doi:10.1007/s10404-006-0147-y.

- [17] K. Mohseni and E. Baird. A unified velocity model for digital microfluidics. Nanoscale and Microscale Thermophysical Engineering, 11(1 & 2):109 – 120, 2007.
- [18] M.G. Pollack, R.B. Fair, and A.D. Shenderov. Electrowetting-based actuation of liquid droplets for microfluidic applications. Appl. Phys. Lett., 77(11):1725–1726, 2000.
- [19] F. Mugele and J.C. Baret. Electrowetting: From basics to applications. Journal of Physics: Condensed Matter, 17(28):R705–R774, 2005.
- [20] C.G. Cooney, C-Y. Chen, A. Nadim, and J.D. Sterling. Electrowetting droplet microfluidics on a single planar surface. Microfluid Nanofluid, DOI: 10.1007/s10404-006-0085-8, 2006.
- [21] E. Baird and K. Mohseni. Digitized heat transfer: A new paradigm for thermal management of compact micro systems. accepted for publication in IEEE Transactions on Components and Packaging Technologies, 2006.
- [22] A. Bejan. Convection Heat Transfer. Wiley-Interscience, United States, 2nd edition, 1994.